Magnetic Resonance Imaging of Plaques in a Cylindrical Channel

Yusuf S. I.[1]*, Aiyesimi Y. M.[1], Jiya M.[1], Awojoyogbe O.B.[2] and Dada O. M.[2]

[1]Department of Mathematics, Federal University of Technology, Minna, Niger State, Nigeria

[2]Department of Physics, Federal University of Technology, Minna, Niger State, Nigeria

*Email: si.yusuf@futminna.edu.ng

Abstract

The detection of blockage in cylindrical pipes using diffusion magnetic resonance equation has been carried out in previous works. In this study, magnetic resonance imaging (MRI) has been employed to image the materials causing fluid blockage in a cylindrical pipe. The Bloch NMR flow equation has been solved analytically in cylindrical coordinates for flow of fluid in a radially symmetric cylindrical pipe. Based on the appropriate boundary conditions, the radial axis was varied to depict blockage in the pipe. The gradient pulse for fluid spin excitation has been designed such that it undergoes exponential rise and fall. The results obtained showed that the graphical pattern changed from vertical orientation (free flow) to horizontal orientation (partial blockage), an indication of presence of materials that may cause obstruction to the fluid. Also, coagulation of colors indicated that obstruction caused is becoming more immense than previously noted. One similarity between the plaques imaged is that as the time is varied, they showed a drop in magnetization. This seems to lay credence to the fact that the model registers signal in its first few seconds or micro-seconds.

Keywords: Bloch NMR diffusion equation, Cylindrical pipe, Plaque, Magnetic resonance imaging.

Correspondence author: *Email: si.yusuf@futminna.edu.ng

Introduction

Magnetic Resonance Imaging (MRI) is a recent approach adopted in the diagnosis of ailments and diseases in humans without surgical invasion. It can also be used to determine problems associated with blockage in cylindrical pipes. It provides accurate assessment of the individual component or multi-component systems in a matter of minutes whereas traditional radioactive tracer techniques may take weeks for each component (Awojoyogbe, *et al.*, 2011). This quick rate of assessment is possible because fluids exhibit random molecular motion of spins. These NMR spins are always in motion, an action that makes them behave like molecular magnets (Yusuf, *et al.,* 2011). The rate of their signal loss or signal attenuation could be easily detected through magnetic resonance coupled with the fact that the molecules of fluids carry magnetic moments with them.

The detected signals usually contain rich fluid flow information and could signify whether or not a problem exists at any point in the flow field. Though not widely known, it has been noted that MRI is capable of quantifying diffusion movement of molecules because of uniqueness in relaxation times - T_1 and T_2 (Yusuf, *et al.*, 2010).

There have been several methods adopted in detecting blockage in fluid pipeline. Yuan *et al.*, (2014) used time splitting algorithms and Godunov mixed format to simulate the pulse propagation in the blocked pipelines. Another technique used by Sattar *et al.*, (2008) is the system frequency response. This is a technique whereby the frequency response is used in the detection of partial blockages in a pipeline. Similar to this is the method adopted by Mohapatra *et al.*, (2006) for the detection of partial blockages in single pipelines by the frequency response method. Wang *et al.*, (2005) also investigated analytically the effects of a partial blockage on pipeline transients. This is done when a partial blockage is simulated using an orifice equation. The influence of the blockage of flow in the unsteady pipe flow is then considered in the equation using a Dirac delta function.

Diffusion Magnetic Resonance Imaging (DMRI), being a viable alternative, is one of the most rapidly evolving techniques in the MRI field. Diffusion and flow can be measured very delicately and accurately using magnetic resonance imaging (Hazlewood *et al.*, 1974). Coefficient of diffusion of a substance defined as the amount of material that diffuses in a certain time plays a vital role in the detection of blockage in a pipe using MRI. Random diffusion motion of water molecules has intriguing properties depending on the physiological and anatomical environment of the organisms being studied. These are the principles being exploited by the method of DMRI.

In this study, we have applied the same principle to radially symmetric cylindrical pipe under the influence of radiofrequency field as a probe to perturb fluid molecules within the pipe. A Radio Frequency (RF) transmitter is needed to transmit energy into the fluid under consideration in the cylinder in order to “activate” the nuclei so that they emit a signal (Waldo and Arnold, 1983). The process undergoes the following four stages: (1) a magnetic field B_0 is applied, (2) the sample responds to B_0 (3) a radio frequency pulse or a train of radio frequencies pulses is applied

during a limited time and (4) the system relaxes. The relaxation process itself is referred to as the free induction decay. The Free Induction Decay (FID) is the time-domain signal obtained during the relaxation process. Summarily, it is the observable NMR signal generated by non-equilibrium nuclear spin magnetization precessing about the magnetic field conventionally along z direction (Hopf *et al.,* 1973), which is analyzed for information mining. This time-domain signal is typically digitized and then Fourier transformed in order to obtain a frequency spectrum of the NMR signal, that is, the NMR spectrum (Duer, 2004).

Methods

Diffusion Magnetic Resonance Equation in Radially Symmetric Cylindrical Pipe

From Yusuf *et al.,* (2015), the diffusion magnetic resonance equation in a radially symmetric cylindrical coordinates is given as:

$$\frac{\partial M_y}{\partial t} = D\left(\frac{\partial^2 M_y}{\partial r^2} + \frac{1}{r}\frac{\partial M_y}{\partial r} + \frac{\partial^2 M_y}{\partial z^2}\right) + \frac{F_o}{T_o}\gamma B_1(t) \quad (1)$$

Equation (1) can be expressed in the form:

$$M_y = F(r,z)U(t) + w_c(t) \quad (2)$$

with $$w_c(\dot{t}) = \frac{F_o}{T_o}\gamma B_1(t) \quad (3)$$

$\Rightarrow$ $$w_c(t) = \int_0^{t_0} \frac{F_o}{T_o}\gamma B_1(t)\, dt \quad (4)$$

Using the method of separation of variables (MSV),

$$M_y = F(r,z)U(t) \quad (5)$$

Hence, the following two differential equations evolve:

$$\frac{dU(t)}{dt} + \lambda^2 DU(t) = 0 \quad (6)$$

$$\frac{\partial^2 F}{\partial r^2} + \frac{1}{r}\frac{\partial F}{\partial r} + \frac{\partial^2 F}{\partial z^2} + \lambda^2 F = 0 \quad (7)$$

By integrating equation (6), the general solution is:

$$U(t) = C_1 e^{-\lambda^2 Dt} \quad \lambda = 1, 2, \ldots, \ldots, \quad (8)$$

where C_1 is the arbitrary constant of integration.

In order to solve (7), the same method of separation of variables is followed:

$$F = Q(r)Z(z) \tag{9}$$

The expression on the right hand side of (9) can be written as a product function of $Q(r)$ and $Z(z)$ only. The first function is in term of (r) and the second function is in term of z only. Both sides must be equal to a constant, say$-\mu^2$, in order to obtain solutions that will not be identically zero. The following two differential equations evolve;

$$\frac{\partial^2 Q}{\partial r^2} + \frac{1}{r}\frac{\partial Q}{\partial r} + \mu^2 Q = 0 \tag{10}$$

and

$$\frac{\partial^2 Z}{\partial z^2} - \beta^2 Z = 0 \tag{11}$$

where we have

$$\beta^2 = \mu^2 - \lambda^2 \tag{12}$$

It could be noted that from equation (10), a Bessel differential equation evolves and its solution is given as

$$F(r) = C_2 J_0(\mu r) + C_3 Y_m(\mu r) \tag{13}$$

where $J_0(\mu r)$ is the Bessel function of the first kind, of order zero and $Y_m(\mu r)$ is the Bessel function of the second kind, of order m. C_2 *and* C_3 are constants.

Also from (11), $$Z(z) = C_4 e^{\beta z} + C_5 e^{-\beta z} \tag{14}$$

Consequently, the solutions to the equations are:

$$U(t) = C_1 e^{-\lambda^2 D t} . \quad \lambda = 1, 2, \ldots, \ldots, \tag{15}$$

$$F(r) = C_2 J_0(\mu r) + C_3 Y_m(\mu r) . \tag{16}$$

$$Z(z) = C_4 e^{\beta z} + C_5 e^{-\beta z} . \tag{17}$$

Combining these solutions for the diffusion Equation (1), this gives the product of the quantities in (15), (16) and (17) plus $\int_0^{t_0} w_c(\dot{t})\, dt$.

$$\Rightarrow \qquad M_y = M_y(r, z, t) = F(r)Z(z)U(t) + \int_0^{t_0} w_c(\dot{t})\, dt \tag{18}$$

$$M_y(r, z, t) = \{C_2 J_0(\mu r) + C_3 Y_m(\mu r)\}\{C_4 e^{\beta z} + C_5 e^{-\beta z}\}\{C_1 e^{-\lambda^2 D t}\} + \int_0^{t_0} w_c(\dot{t})\, dt \tag{19}$$

Initial and Boundary Conditions to Determine Blockage of Fluid at any Point in a Cylindrical Geometry Using Diffusion Magnetic Resonance Equation

In order to examine the behaviour of fluid flow at the point of blockage, the initial and boundary conditions used by Spiegel (1974) for heat flow to determine the temperature of molecules of fluid at any point in cylinder will now be adopted to determine the magnetization of fluid at the

point of blockage using the diffusion equation. The nature of the blockage which could be partial or total will then be examined. The boundary conditions are:

$$i)\ M_y(r,z,0) = M_i(r,z);$$

$$ii)\ M_y(r,0,t) = 0;$$

$$iii) M_y(r,L,t) = 0;$$

$$iv) M_y(a,z,t) = 0;$$

$$v)\left|M_y(r,z,t)\right| < M,$$

$$M = 1,2,3 \ldots i.e. positive\ integers \qquad (20)$$

where r *is the space depicting the blockage* and z is the direction of flow and both are defined as

$$0 \le r < a; \quad 0 < z < L; \quad t > 0$$

The boundary conditions are now applied in evolving the model equation that will be used to determine the blockage in the cylinder.

Firstly, $r = 0, Y_m(\mu r) \to -\infty$; to keep the solution finite, C_3 must be zero. Thus the solution becomes

$$\Rightarrow \qquad M_y(r,z,t) = \left\{e^{-\lambda^2 Dt}\right\}\{C_2 J_0(\mu r)\}\{C_4 e^{\beta z} + C_5 e^{-\beta z}\} \qquad (21)$$

From the second boundary condition, we see that

$$M_y(r,0,t) = \left\{e^{-\lambda^2 Dt}\right\}\{J_0(\mu r)\}\{C_4 + C_5\} = 0 \qquad (22)$$

So that we must have $C_4 + C_5 = 0$ implying that $C_5 = -C_4$

then (21) becomes

$$M_y(r,z,t) = \left\{e^{-\lambda^2 Dt}\right\}\{J_0(\mu r)\}\{e^{\beta z} - e^{-\beta z}\} = 0 \qquad (23)$$

From the third condition, we have

$$M_y(r,L,t) = \left\{e^{-\lambda^2 Dt}\right\}\{J_0(\mu r)\}\{e^{\beta L} - e^{-\beta L}\} = 0 \qquad (24)$$

which can be satisfied with $e^{\beta L} - e^{-\beta L} = 0$,

$$\Rightarrow e^{\beta L}.e^{\beta L} = e^{-\beta L}.e^{\beta L} = 1 = e^{2k\pi i} \qquad (25)$$

Note that $$e^{ix} = cosx + isinx \qquad (26)$$

and that implies $$e^{2\pi i} = cos2\pi + isin2\pi = 1 = e^{2k\pi i}.\ k = 0,1,2, \ldots \ldots \qquad (27)$$

$$\therefore e^{2\beta L} = e^{2k\pi i} \qquad k = 0,1,2, \ldots \ldots \qquad (28)$$

It follows that we must have $2\beta L = 2k\pi i$

or $$\beta = \frac{k\pi i}{L}, \qquad k = 0, 1, 2, \ldots \ldots \tag{29}$$

Using this in (23), it becomes

$$M_y(r, L, t) = \left\{Ce^{-\lambda^2 Dt}\right\}\{J_0(\mu r)\}sin\frac{k\pi z}{L} = 0 \tag{30}$$

where C is a new constant.

From the fourth condition, we obtain

$$M_y(a, z, t) = \left\{Ce^{-\lambda^2 Dt}\right\}\{J_0(\mu a)\}sin\frac{k\pi z}{L} = 0 \tag{31}$$

which can be satisfied only if

$$\{J_0(\mu a)\} = 0 \tag{32}$$

$$\mu a = s_1, s_2, \ldots. \tag{33}$$

$$\mu = \frac{s_1}{a}, \frac{s_2}{a}, \ldots. \tag{34}$$

where $\frac{s_m}{a}(m = 1,2, \ldots .)$is the positive root of the Bessel function $\{J_0(x)\} = 0$.

Now from (12), (29) and (34), it follows that:

$$\lambda^2 = (\frac{s_m}{a})^2 - (\frac{k\pi i}{L})^2 \ = (\frac{s_m}{a})^2 + (\frac{k\pi}{L})^2 \tag{35}$$

so that a solution satisfying all the boundary conditions except the first is given by

$$M_y(r, z, t) = \left\{Ce^{-Dt(\frac{s_m}{a})^2 + (\frac{k\pi}{L})^2}\right\}\left\{J_0\left(\frac{s_m}{a}r\right)\right\}sin\frac{k\pi z}{L} \tag{36}$$

where $k = 1,2,3, \ldots ..; m = 1,2,3, \ldots.$

Replacing $C\ by\ C_{km}$ and summing over $k\ and\ m$ we obtain by the superposition principle the solution

$$M_y(r, z, t) = \sum_{k=1}^{\infty}\sum_{m=1}^{\infty}\left\{C_{km}e^{-Dt(\frac{s_m}{a})^2 + (\frac{k\pi}{L})^2}\right\}\left\{J_0\left(\frac{s_m}{a}r\right)\right\}sin\frac{k\pi z}{L} \tag{37}$$

The first condition in (3.68) now leads to

$$M_i\,(r, z) = \sum_{k=1}^{\infty}\sum_{m=1}^{\infty}\{C_{km}\}\left\{J_0\left(\frac{s_m}{a}r\right)\right\}sin\frac{k\pi z}{L} \tag{38}$$

This can be written as

$$M_i(r,z) = \sum_{k=1}^{\infty}[\sum_{m=1}^{\infty}\{C_{km}\}\left\{J_0\left(\frac{S_m}{a}r\right)\right\}]sin\frac{k\pi z}{L} = \sum_{k=1}^{\infty} b_k sin\frac{k\pi z}{L} \quad (39)$$

$$\Rightarrow \quad b_k = \sum_{m=1}^{\infty}\{C_{km}\}\left\{J_0\left(\frac{s_m}{a}r\right)\right\} \quad (40)$$

It follows from this that b_k are the Fourier coefficients obtained when $M_i(r,z)$ is expanded into a Fourier sine series in z (r being kept constant).

Thus

$$b_k = \frac{2}{L}\int_0^1 M_i(r,z)sin\frac{k\pi z}{L}dz \quad (41)$$

We now find C_{km} from the expansion in equation (39). Since $b_k$is a function of r this is simply the expansion of b_k into a Bessel series.

Consequently,

$$C_{km} = \frac{2}{J_1^2\left(\frac{S_m}{a}\right)}\int_0^1 r b_k J_0\left(\frac{S_m}{a}r\right)dr \quad (42)$$

Using (40),

$$C_{km} = \frac{4}{J_1^2\left(\frac{S_m}{a}\right)L}\int_0^1\int_0^1 r M_i(r,z)J_0\left(\frac{S_m}{a}r\right)sin\frac{k\pi z}{L}drdz \quad (43)$$

The required solution is

$$M_y(r,z,t) = \sum_{k=1}^{\infty}\sum_{m=1}^{\infty}\left\{C_{km}e^{-Dt(\frac{S_m}{a})^2+(\frac{k\pi}{L})^2}\right\}\left\{J_0\left(\frac{S_m}{a}r\right)\right\}sin\frac{k\pi z}{L} \quad (44)$$

with C_{km}in (42) as coefficient.

With the radio frequency (rf) field, the solution becomes

$$M_y(r,z,t) = \sum_{k=1}^{\infty}\sum_{m=1}^{\infty}\left\{C_{km}e^{-Dt(\frac{S_m}{a})^2+(\frac{k\pi}{L})^2}\right\}\left\{J_0\left(\frac{S_m}{a}r\right)\right\}sin\frac{k\pi z}{L} + \frac{aF_o}{wT_o}\gamma\sin(wt) \quad (45)$$

Assume $M_i(r,z) = \sigma_0$, a constant.

$$C_{km} = \frac{4\sigma_0}{J_1^2\left(\frac{S_m}{a}\right)}\int_0^1\int_0^1 r J_0\left(\frac{S_m}{a}r\right)sin\frac{k\pi z}{L}drdz \quad (46)$$

$$C_{km} = \frac{4\sigma_0}{J_1^2(\frac{S_m}{a})L}\{\int_0^1 rJ_0\left(\frac{s_m}{a}r\right)dr \int_0^1 sin\frac{k\pi z}{L}dz \quad (47)$$

$$= \frac{4\sigma_0}{J_1^2\left(\frac{S_m}{a}\right)}\left\{\frac{J_1\left(\frac{S_m}{a}\right)}{\frac{S_m}{a}}\right\}\left\{\frac{1-cosk\pi}{k\pi}\right\} \quad (48)$$

$$= \frac{4\sigma_0(1-cosk\pi)}{k\pi\frac{S_m}{a}J_1\left(\frac{S_m}{a}\right)} \quad (49)$$

Substituting for C_{km} in equation (44)

$$M_y(r,z,t) = \frac{4\sigma_0}{\pi}\sum_{k=1}^{\infty}\sum_{m=1}^{\infty}\left\{\frac{(1-cosk\pi)}{k\pi\frac{S_m}{a}J_1\left(\frac{S_m}{a}\right)}e^{-Dt(\frac{S_m}{a})^2+(\frac{k\pi}{L})^2)}\right\}\left\{J_0\left(\frac{S_m}{a}r\right)\right\}sin\frac{k\pi z}{L} \quad (50)$$

The Radio Frequency (RF) Field

The Radio Frequency (RF) transmitter is needed to transmit energy into the sample of the fluid under consideration in the cylinder in order to "activate" the nuclei so that they emit a signal. The transmitter coil applies to the sample an RF magnetic field $\boldsymbol{B_1(t)}$ where $\boldsymbol{B_1(t)} = bB_1(t)coswt$. Such a field is said to be linearly polarized, since it oscillates in a single direction. *w* is called the irradiation frequency; it is also the reference frequency of the RF transmitter and the detection system. *w* has value - $1x10^8$ rad. s^{-1} (Waldo and Arnold, 1983).
Therefore, to find the solution of

$$w_c(t) = \int_0^{t_0}\frac{F_o}{T_p}\gamma B_1(t)\,dt \quad (51)$$

the radio frequency field (rf) is defined as

$$\boldsymbol{B_1(t)} = bB_1(t)coswt \quad (52)$$

$$\Rightarrow w_c(t) = \int_0^{t_0}\frac{F_o}{T_p}b\gamma B_1(t)coswt\,dt \text{ where } F_o = \frac{M_o}{T_1} \text{ and } T_p = \frac{1}{T_1}+\frac{1}{T_2} \quad (53)$$

Consequently,

$$\int_0^{t_0}\frac{bF_o}{T_p}\cos(wt)\,dt = \frac{bF_o}{wT_p}\gamma\sin(wt) \quad (54)$$

Finally, the solution for the magnetization M_y, of any molecule of the fluid at any point (r,z,t) in the cylinder is given as

$$M_y(r,z,t) = \frac{4\sigma_0}{\pi}\sum_{k=1}^{\infty}\sum_{m=1}^{\infty}\left\{\frac{(1-cosk\pi)}{k\frac{S_m}{a}J_1(\frac{S_m}{a})}e^{-Dt(\frac{S_m}{a})^2+(\frac{k\pi}{L})^2}\right\}\left\{J_0\left(\frac{S_m}{a}r\right)\right\}sin\frac{k\pi z}{L} + \frac{bF_o}{wT_p}\gamma\sin(wt) \quad (55)$$

where the diffusion coefficient $D = -\frac{V^2}{T_p}$ was accurately defined in terms of MRI flow parameters fluid velocity, v, T_1 and T_2 relaxation rates (as $T_p = \frac{1}{T_1}+\frac{1}{T_2}$), $s_m = \gamma G\delta$ and $F_0 = \frac{M_0}{T_1}$, γ = gyromagnetic ratio, RF = gradient pulse magnitude and δ = gradient pulse duration. J_0 is the Bessel function of the first kind (order 0), J_1 is the Bessel function of the first kind (order 1), σ_0 is a function of the equilibrium magnetization while *a* is the radius of the pipe.

From equation (55), the transverse magnetization is given as follows:

$$M_y(r,z,t) = \frac{4\sigma_0}{\pi}\sum_{k=1}^{\infty}\sum_{m=1}^{\infty}\left\{\frac{(1-cosk\pi)}{k\frac{S_m}{a}J_1(\frac{S_m}{a})}e^{-Dt(\frac{S_m}{a})^2+(\frac{k\pi}{L})^2}\right\}\left\{J_0\left(\frac{S_m}{a}r\right)\right\}sin\frac{k\pi z}{L} + \frac{F_o}{T_p}\int_{\delta}^{t}\gamma B_1(t)\mathrm{dt} \quad (56)$$

If the radio frequency (RF) magnetic field is defined as follows (Price, 1997; 1998):

$$B_1(t) = G(t)r \quad (57)$$

Therefore, the integral in equation (56) becomes:

$$\frac{F_o}{T_p}\int_{\delta}^{t}\gamma B_1(t)\mathrm{dt} = \frac{T_2M_0r}{T_1+T_2}\int_{\delta}^{t}G(t)\mathrm{dt} \quad (58)$$

If it is assumed that the gradient pulse $G(t)$**,** is designed such that $G(t)$ under goes exponential rise and fall (Price, 1997, 1998 and Dada *et al.,* 2015), then we have:

$$G(t) = g\exp\left(-\frac{t}{T_1+T_2}\right) \quad (59)$$

where g is the magnitude of the gradient pulse and δ is the gradient pulse duration. The integral in equation (58) becomes:

$$\frac{F_o}{T_p}\int_{\delta}^{t}\gamma B_1(t)\mathrm{dt} = \frac{T_2M_0r}{T_1+T_2}(T_1+T_2)g\exp\left(\frac{(t-\delta)}{T_1+T_2}\right) = -gT_2M_0r\exp\left(\frac{(t-\delta)}{T_1+T_2}\right) \quad (60)$$

Using equation (60) and setting $k = 1$, equation (56) becomes:

$$M_y(r,z,t) = \frac{4\sigma_0}{\pi}\sum_{m=1}^{\infty}\left\{\frac{(1-\cos\pi)}{\frac{s_m}{a}J_1\left(\frac{s_m}{a}\right)}\exp\left(-Dt\left(\frac{s_m}{a}\right)^2+\left(\frac{\pi}{L}\right)^2\right)\right\}\left\{J_0\left(\frac{s_m}{a}r\right)\sin\left(\frac{\pi z}{L}\right)\right\} - gT_2M_0r\exp\left(-\frac{(t-\delta)}{T_1+T_2}\right) \tag{61}$$

$$M_y(r,z,t) = \frac{8\sigma_0}{\pi}\sum_{m=1}^{\infty}\left\{\frac{1}{\frac{s_m}{a}J_1\left(\frac{s_m}{a}\right)}\exp\left(-Dt\left(\frac{s_m}{a}\right)^2+\left(\frac{\pi}{L}\right)^2\right)\right\}\left\{J_0\left(\frac{s_m}{a}r\right)\sin\left(\frac{\pi z}{L}\right)\right\} - gT_2M_0r\exp\left(-\frac{(t-\delta)}{T_1+T_2}\right) \tag{62}$$

where L is the length of pipe used.

For simulation, we consider oil wax and oil based mud as two materials responsible for blockages in the pipe. Given that T_1 and T_2 are the relaxation times of the fluid conditions within the pipe, as shown in table 1:

Material	**T_1 (s)**	**T_2 (s)**	**D (cm^2s^{-1})**	**D (m^2s^{-1})**
Oil	0.84	0.325	0.0000052	5.2E-10
Crude oil	0.5	0.486	0.000002	2.0E-10
Oil wax	1.1195	0.5432	0.0000035	3.5E-10

Table 1: Fluid Properties of Oil, Crude oil and Oil wax

NMR fluid properties at reservoir conditions are B_0 = 0.0176T, *TE* = 1.2 ms, *G* = 18 gauss/cm (Coates *et al*., 1999) where $B_0$is the static field; G is the gradient field and TE is the echo time. In order to improve the contrast of the imaging method proposed in this study, we shall modify the definition of S_m as follows:

$$S_m = \frac{T_1}{T_2}\gamma g\delta(FOV) \tag{63}$$

where FOV is the field of view, g is the gradient pulse magnitude and δ is the gradient pulse duration. This expression indicates that the selection of a value for the index m translates into

choosing an observed set of relaxation times. Since σ_o is a constant, it can be assumed that $\sigma_o = M_o$, Equation (62) for just a given set of relaxation times becomes:

$$M_y(r,z,t)|_{r_1 r_2} = \frac{8M_o}{\pi}\left\{\frac{1}{\left(\frac{T_1}{aT_2}\gamma g\delta(FOV)\right)J_1\left(\frac{T_1}{aT_2}\gamma g\delta(FOV)\right)}\exp\left[-Dt\left(\frac{T_1}{aT_2}\gamma g\delta(FOV)\right)^2 + \left(\frac{\pi}{L}\right)^2\right]\left\{J_o\left(\frac{T_1}{aT_2}\gamma g\delta(FOV)r\right]\sin\left(\frac{\pi z}{L}\right)\right\} - gT_2M_o r\exp\left(-\frac{(t-\delta)}{T_1+T_2}\right) \quad (64)$$

Results

Imaging of Flow of Oil with Lateral Adjustments

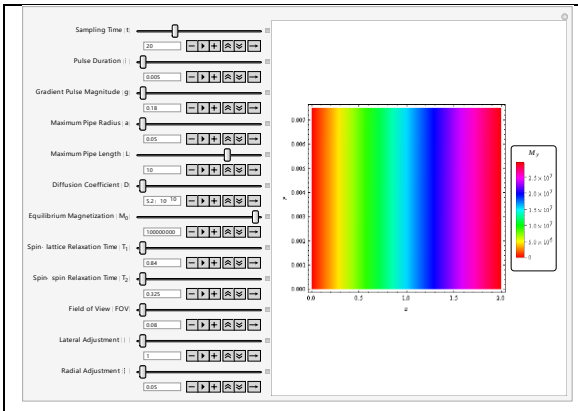

Figure 1a: Imaging of blockage with lateral adjustment = 1 and radial adjustment = 0.05

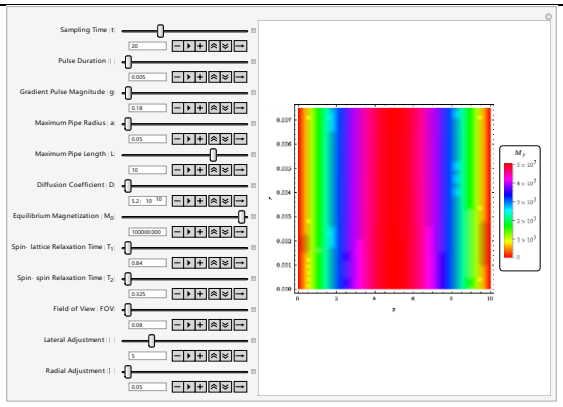

Figure 1b: Imaging of blockage with lateral adjustment = 5 and radial adjustment = 0.05

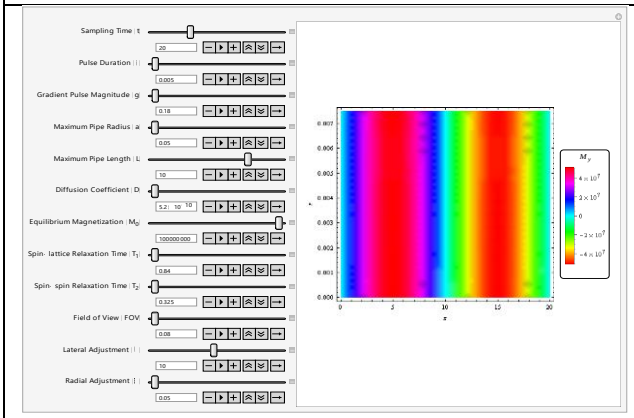

Figure 1c: Imaging of blockage with lateral adjustment = 10 and radial adjustment = 0.05

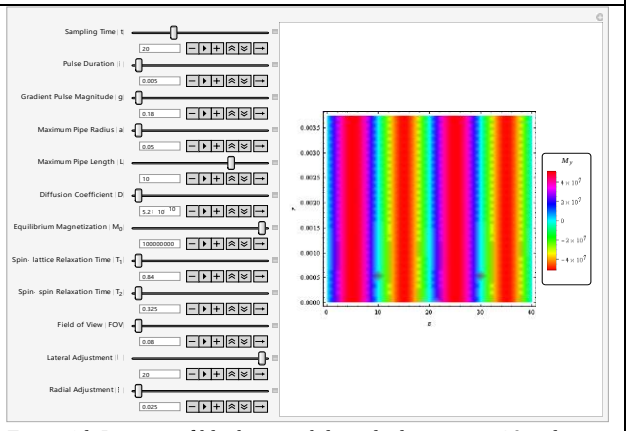

Figure 1d: Imaging of blockage with lateral adjustment = 20 and radial adjustment = 0.025

Imaging of Flow of Oil with Radial Adjustment

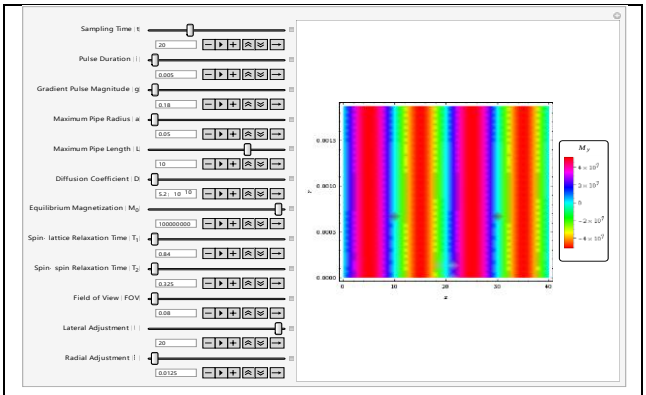

Figure 2a: Imaging of blockage with lateral adjustment = 20 and radial adjustment = 0.0125

Imaging of Flow of Oil with Time Adjustment

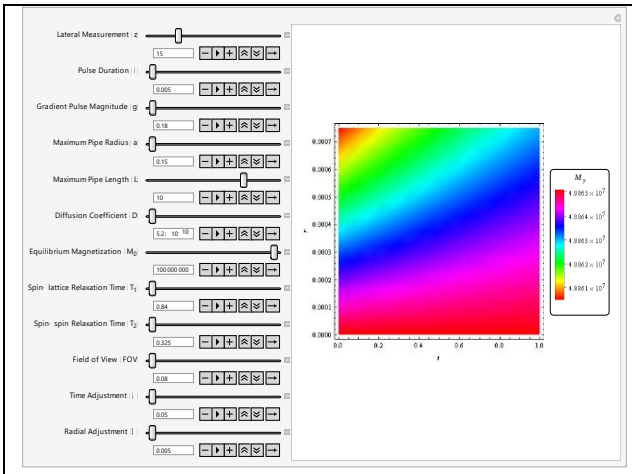

Figure 3a: Imaging of blockage with time adjustment = 0.05 and radial adjustment = 0.05

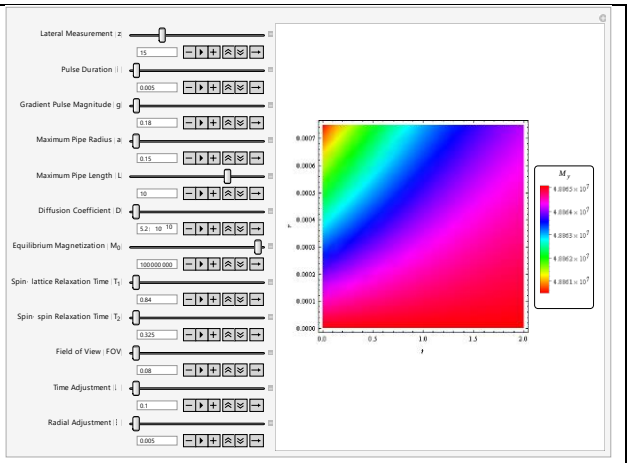

Figure 3b: Imaging of blockage with time adjustment = 0.1 and radial adjustment = 0.05

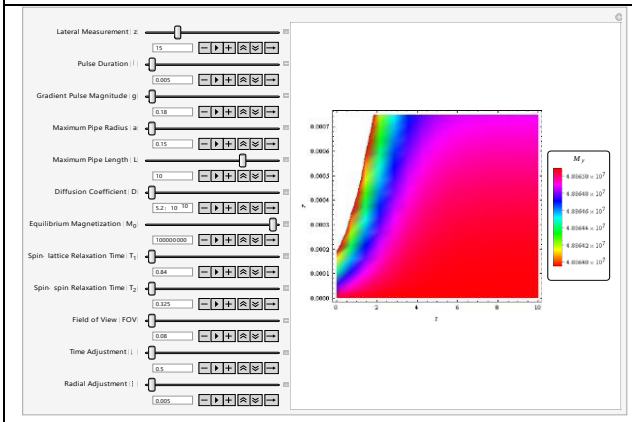

Figure 3c: Imaging of blockage with time adjustment = 0.5 and radial adjustment = 0.05

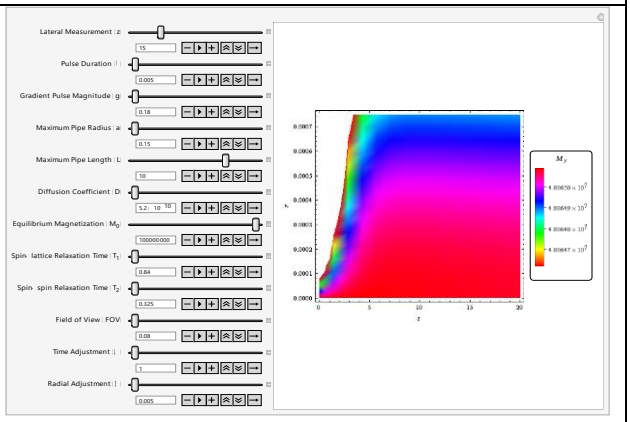

Figure 3d: Imaging of blockage with time adjustment = 1 and radial adjustment = 0.05

Imaging of Oil Wax as a Causative Agent of Blockage with Time Adjustment

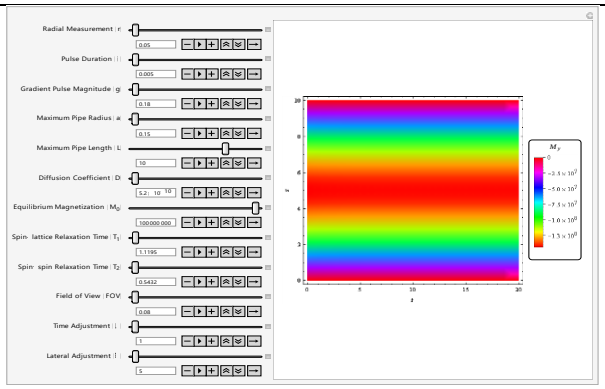

Figure 4a: Imaging of blockage with time adjustment =5 and radial adjustment = 0.005 for oil wax

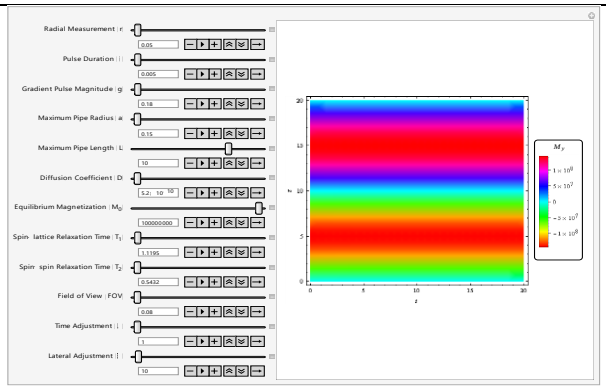

Figure 4b: Imaging of blockage with time adjustment =10 and radial adjustment =0.005 for oil wax

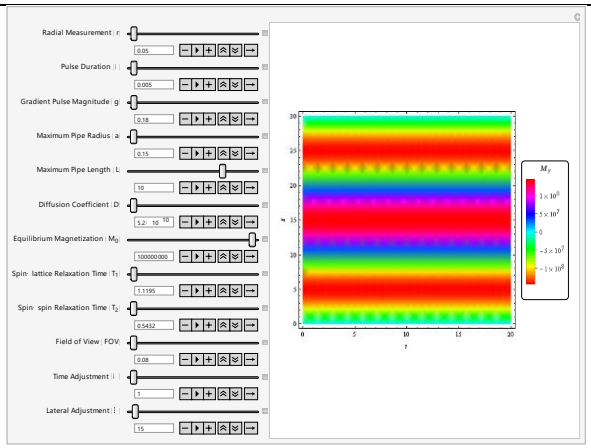

Figure 4c: Imaging of blockage with time adjustment = 15 and radial adjustment = 0.005 for oil wax

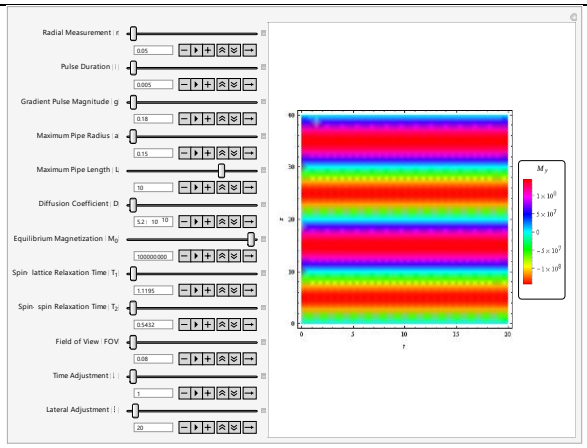

Figure 4d: Imaging of blockage with time adjustment = 20 and radial adjustment = 0.005 for oil wax

Imaging of Oil Based Mud (OBM) as a Causative Agent of Blockage with Time Adjustment

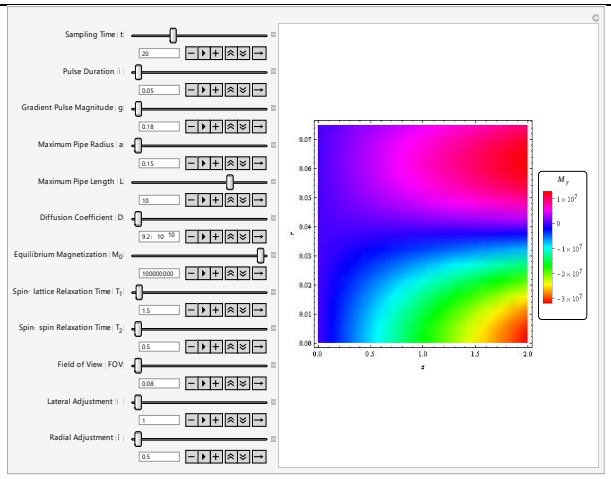

Figure 5a: Imaging of blockage with lateral adjustment = 1 and radial adjustment = 0.5 for mud

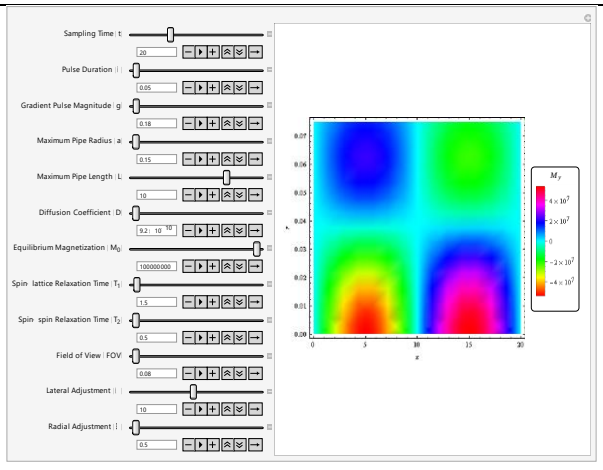

Figure 5b: Imaging of blockage with lateral adjustment =10 and radial adjustment = 0.5 for mud

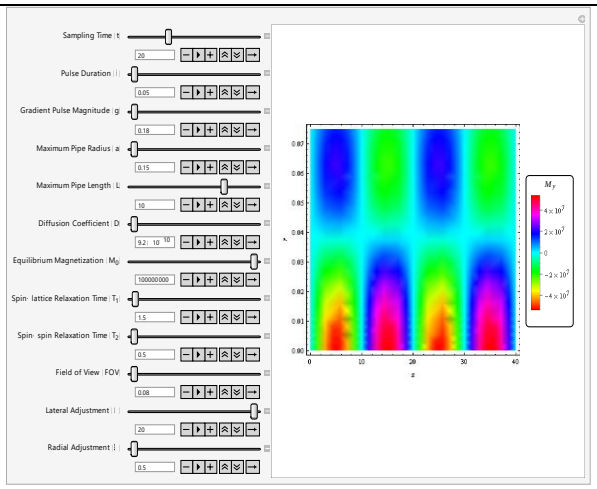

Figure 5c: Imaging of blockage with lateral adjustment = 20 and radial adjustment = 0.5 for mud

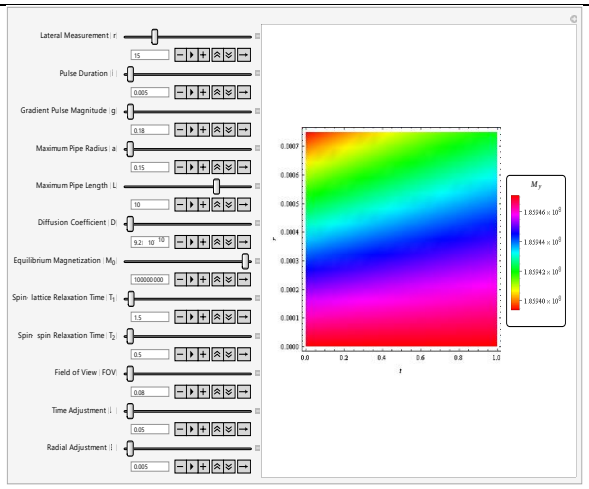

Figure 5d: Imaging of blockage with time adjustment = 0.05 and radial adjustment = 0.005 for mud

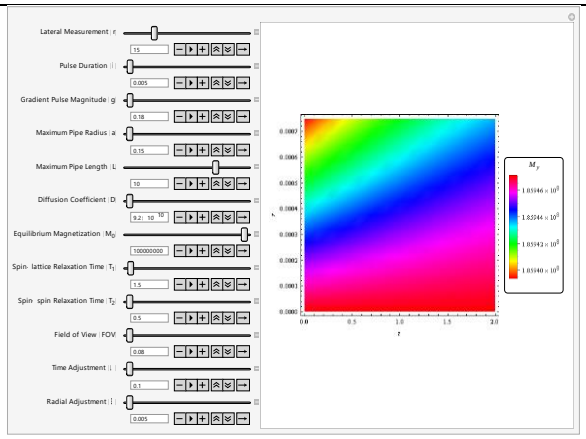

Figure 5e: Imaging of blockage with time adjustment = 0.1 and radial adjustment = 0.005 for mud

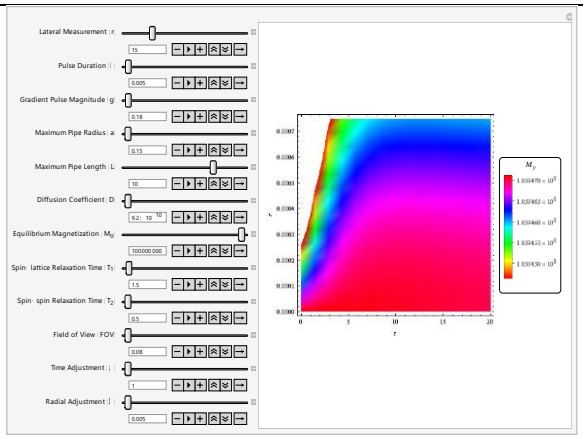

Figure 5f: Imaging of blockage with time adjustment =1 and radial adjustment = 0.005 for mud

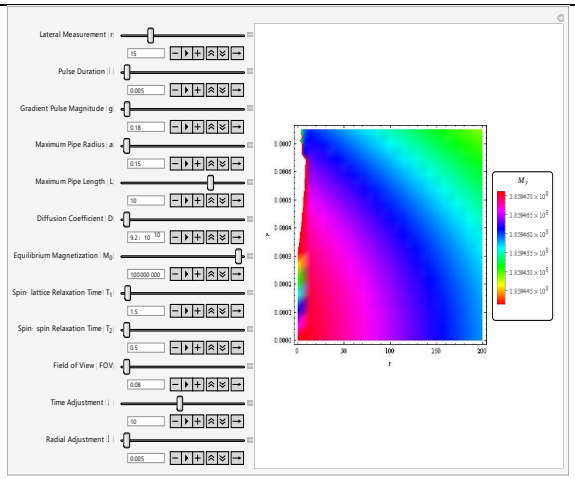

Figure 5g: Imaging of blockage with time adjustment =10 and radial adjustment =0.005 for mud

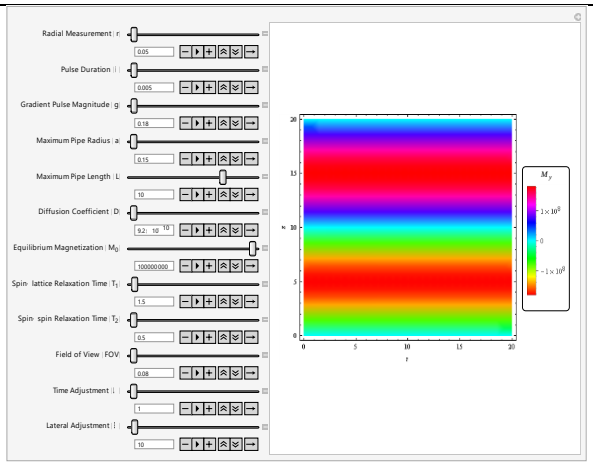

Figure 5h: Imaging of blockage with time adjustment =1 and lateral adjustment =10 for mud

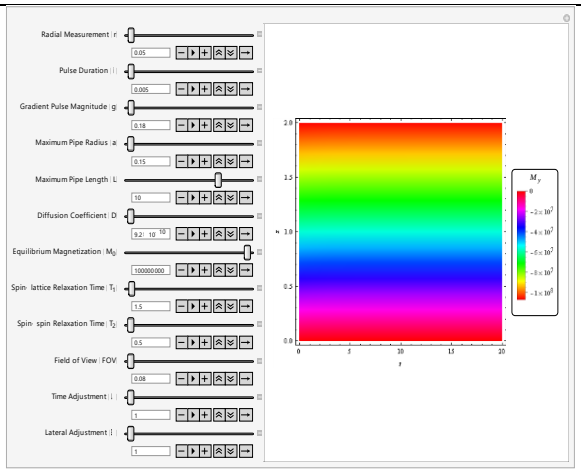

Figure 5i: Imaging of blockage with time adjustment =1 and lateral adjustment =1 for mud

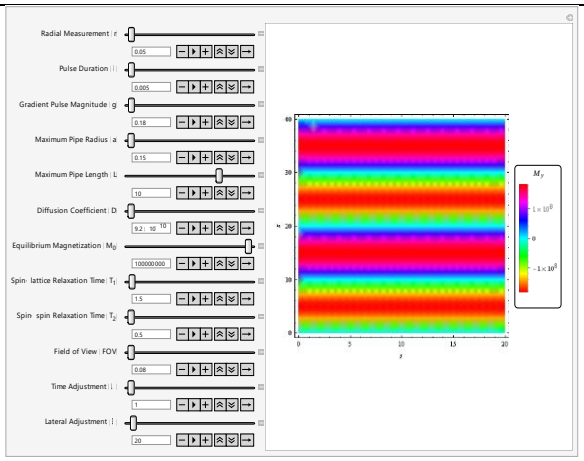

Figure 5j: Imaging of blockage with time adjustment =1 and lateral adjustment = 20 for mud

Discussion of Results

From equation (62) and the use of the relaxation parameters in Table 1, the possibility of performing computational MRI to image different components of obstruction or blockage in cylindrical pipe has been clearly demonstrated. Unique images for oil, crude oil and wax were obtained. It would be observed that the images from oil are quite similar when values were varied laterally and radially (Figure 1a-d and 2a). They have vertical orientation, an indication of free flow condition of the fluid within the cylindrical pipe.

However, from Figures 3a-3d and 4a-4d, the pattern changed from vertical to horizontal orientation with oil wax recording an initial negative magnetization. This is an indication of presence of materials that may cause obstruction to fluid flow. More conspicuous is the pattern demonstrated by plots from the oil-based mud (figures 5a-5j). This coagulation of colors indicates that obstruction caused by mud could be more immense than that from oil wax.

Conclusion

Magnetic resonance imaging has been used to image the materials causing the blockage of fluid in a cylindrical pipe. The gradient pulse for fluid spin excitation has been designed such that it undergoes exponential rise and fall. One similarity between the two blockages imaged is that as the time is varied, they both showed a drop in transverse magnetization. This seems to lay credence to the fact that the model registers signal in its first few seconds or micro-seconds.

What is interesting in this work is that few NMR data are required for blockage imaging and the computational model is capable of interpolating for data points which are impossible to image directly because of NMR hardware restrictions.

Acknowledgment

Management of the Federal University of Technology, Minna is hereby acknowledged for sponsoring this research work.

References

Awojoyogbe, O. B., Faromika, O. P., Dada, M. and Dada, O.E. (2011). Mathematical Concepts of the Bloch Flow Equations for General Magnetic Resonance Imaging: *Concepts in Magnetic Resonance Part A*, Vol. 38A (3) 85-101.

Coates, G. R., Xiao, L. and Prammer, G. M. (1999). NMR Logging Principles and Applications. *Halliburton Energy Services;* Houston, USA.

Dada, O. M., Awojoyogbe, O. B. and Ukoha, A. C. (2015). A Computational Analysis for Quantitative Evaluation of Petrol-Physical Properties of Rock Fluids Based on Bloch NMR Diffusion Model for Porous media. *Journal of Petroleum Science and Engineering* 127, 137 – 147.

Duer, M. J. (2004). Introduction to Solid-State NMR Spectroscopy. *Blackwell Publishing*: Oxford, p. 43-58.

Hazlewood, C. F., Chang, D. C. and Nichols, B. L. (1974). Nuclear Magnetic Resonance Relaxation Times of Water Protons in Skeletal Muscle, *Journal of Biological Physics* 14: 583-606.

Hopf, F. A., Shea, R. F., & Scully, M. O. (1973). Theory of optical free-induction decay and two-photon superradiance. *Physical Review A*, *7*(6), 2105–2110.

Mohapatra, P., Chaudhry, M., Kassem, A., and Moloo, J. (2006). Detection of Partial Blockage in Single Pipelines. *Journal of Hydraulic Engineering*, 132(2), 200–206.

Price, W. S. (1997). Pulsed-field gradient nuclear magnetic resonance as a tool for studying translational diffusion: Part I. Basic theory. *Concepts in Magnetic Resonance Part A*, *9*(5), 299-336.

Price, W. S. (1998). Pulsed-field gradient nuclear magnetic resonance as a tool for studying translational diffusion: Part II. Experimental aspects. *Concepts in Magnetic Resonance Part A, 10*(4), 197-237.

Sattar, A., Chaudhry, M., and Kassem, A. (2008). Partial Blockage Detection in Pipelines by Frequency Response Method. *Journal of Hydraulic Engineering*, 134(1), 76–89.

Torrey, H. C. (1956). Bloch equations with diffusion terms. *Physical Review*; 104 (3): 563-565.

Waldo, S. Hinshaw and Arnold H. Lent **(**1983**).** An Introduction to NMR Imaging: From the Bloch Equation to the Imaging Equation. *Proceedings of the IEEE,* vol. 71, no. 3.

Wang, X., Lambert, M., and Simpson, A. (2005). "Detection and Location of a Partial Blockage in a Pipeline Using Damping of Fluid Transients." *Journal of Water Resources, Planning and Management*, 131(3), 244–249.

Yuan Tian, Xuefen Zhao, Dan Tian, Rui Wu and Huan Tang (2014). Applied Mechanics and Materials Vols 490-491 pp 490-497. *TransTech Publications, Switzerland Doi:10.4028/www.scientific.net/AMM.490-491.490*.

Yusuf, S. I., Aiyesimi, Y. M., Jiya, M. and Awojoyogbe, O. B. (2015). Detection of Blockage in a Radially Symmetric Cylindrical Pipe using Diffusion Magnetic Resonance Equation. *Journal of Science, Technology, Mathematics and Education;* 11(3), 192 – 200.

Yusuf, S. I., Aiyesimi Y. M. and Awojoyogbe, O. B. (2010). An Analytic Investigation of Bloch Nuclear Magnetic Resonance Flow Equation for the Analysis of General Fluid Flow, *Nigerian Journal of Mathematics and Applications* Vol. 20: 82 – 92.

Yusuf, S. I., Aiyesimi, Y. M. and Awojoyogbe, O. B. (2011). Effect of Transverse Relaxation Rates on Time-Dependent Magnetic Resonance Imaging, *African Journal of Physical Sciences* Vol. 4(1): 119 – 126.